GEOPHYSICAL RESEARCH LETTERS, VOL. 27, NO. 16, PAGES 2473-2476, AUGUST 15, 2000

Improving the Abel inversion by adding ground GPS data to LEO radio occultations in ionospheric sounding

M. Hernández-Pajares, J. M. Juan and J. Sanz

Group of Astronomy and Geomatics, Universitat Politècnica de Catalunya, Barcelona, Spain

Abstract. GPS radio occultations allow the sounding of the Earth's atmosphere (i.e. troposphere and ionosphere). The basic observable of this technique is the additional delay, due to the refractivity index, of a radio signal when passing through the atmosphere. This additional delay is proportional to the integrated refractivity, in such a way that we can obtain an estimation of the vertical refractivity profiles using observations at different elevation angles by solving an inverse problem. Traditionally, the solution of this inverse problem is obtained by using the Abel inversion algorithm assuming a refractivity index that only depends on the altitude. In this paper we present a modified Abel inversion algorithm for ionospheric sounding that overcomes the spherical symmetry assumption of the traditional Abel inversion algorithm. Processing a set of simulated data and 1 day of real data with this algorithm, a clear improvement over the traditional one can be obtained when comparing the derived critical frequencies with the ionosonde measurements. It is also shown that this improvement is sufficient to measure critical frequencies associated with the ionospheric E layer.

Introduction

In recent years several authors have used GPS radio occultations (i.e. signals received at negative elevations) from a receiver on board a low Earth orbit (LEO) satellite to obtain vertical ionospheric profiles (VIP). The procedures used to obtain VIP can be classified into two main groups: (i) the tomographic approach (*Leitinger et al.*, 1997, *Hernandez-Pajares et al.*, 1998), which involves using a set of orthogonal functions to describe the electron density, and (ii) the Abel transform (*Hardy et al.*, 1993, *Hajj et al.*, 1998, *Schreiner et al.*, 1999), which provides directly the electron density from either the bending angle of the LEO-GPS ray or the excess of phase data of the signal (proportional to the slant total electron content, STEC).

The tomographic approach also requires data from ground receivers that take into account the horizontal gradient in the electron density. Usually, this approach involves estimating a large number of parameters and results in a low vertical resolution. In comparison, the Abel inversion has a simpler performance and a better vertical resolution (depending on the data sampling rate). However, two major assumptions are necessary in order to use the traditional Abel inversion technique. The first one is that the electron distribution must present spherical symmetry (i.e. the electron density only depends on height). However, when a LEO-GPS ray passes through the ionosphere the ionospheric delay could be caused by points with horizontal distances of ten degrees or more (more than 1000 km), so two points with the same height could have clearly different densities. The second assumption is that the electron density above the LEO can be neglected. This assumption, which mainly affects the estimation of the outer point densities, can be overcome by: (i) calculating the ionospheric delay above the LEO from observations with positive elevations (this can be done if spherical symmetry is supossed, *Schreiner et al.*, 1999) or (ii) extrapolating above the LEO height either the data (*Hajj et al.*, 1998) or, as we do in this work, the VIP in an iterative process (described below).

In order to avoid the spherical symmetry assumption, *Hajj el al.* (1994) proposed a tomographic inversion including 3-D constraints and solving for a scale factor that depends on height. *Schreiner et al.* (1999) used this method by constraining the tomographic inversion with a priori electron densities obtained in three different ways. They conclude that these constrained inversions offer no improvement over the classical Abel inversion with the spherical symmetry hypothesis.

In this paper we present a modified Abel algorithm (similar to the algorithm proposed by *Hajj et al.*, 1994) that overcomes the spherical symmetry hypothesis by using the vertical electron content (TEC) as constraint.

The inversion algorithm

For a given occultation we can write the STEC of each ray i as a function of its *impact parameter* p_i (see Figure 1). In this way, for all rays in the occultation, a set of spherical shells like "onion rings" can be constructed (*Leitinger et al*, 1997), where the mean radius of the shell is the impact parameter of the ray.

The STEC is related to the electron density N_e by:

$$STEC(p) = \int_{LEO}^{GPS} N_e \cdot dl \qquad (1)$$

At this point we suppose that the electron density is separable (separability hypothesis):

$$N_e(LT, \Phi, H) = TEC(LT, \Phi) \cdot F(H) \qquad (2)$$

where LT is the local time coordinate, Φ is the latitude, H is the height, TEC is the vertical total electron content at a point with horizontal coordinates (LT, Φ) and F is a shape (scaling) function. Taking into account that the TEC function is the integrated electron density in a vertical direction, $F(h)$ must verify:

$$\int_0^\infty F(H) \cdot dH = 1 \qquad (3)$$

Paper number 2000GL000032.
0094-8276/00/2000GL000032$05.00

Table 1. Fractional differences between ionosonde frequencies and occultation derived frequencies. In each column the first sub-column corresponds to the separability hypothesis and the second sub-column to the spherical symmetry hypothesis.

	Internal comparisons		foF2 all LT		foF2 no dawn occ.		foF2 dawn occ.		foE	
	Sep.	Sph.	Sep.	Sph.	Sep.	Sph.	Sep.	Sph.	Sep.	Sph.
# comparisons	30	30	114	114	90	90	24	24	16	16
mean (%)	-0.9	-3.8	1.6	0.3	0.0	-1.8	7.8	8.3	-4.2	-14.8
rms (%)	11.0	22.2	8.8	14.1	6.9	11.2	13.6	21.5	15.0	21.0

This formulation for the electron density does not complicate the model excessively because the TEC function can be easily computed from ground receiver data (see, for example, *Hernandez-Pajares et al.*, 1999).

Starting from the outer ray ($p_1 = r_{LEO}$) , for a given ray i, where $i = 1...$, with impact parameter, p_i, its $STEC$ can be written in a discrete representation as (see Figure 1):

$$STEC(p_i) = 2 \cdot l_{ii} \cdot TEC(LT_{ii}, \Phi_{ii}) \cdot F(p_i) + \sum_{j=1}^{j=i-1} l_{ij} \left[TEC(LT_{ij}, \Phi_{ij}) + TEC(LT'_{ij}, \Phi'_{ij}) \right] F(p_j) \quad (4)$$

where LT_{ij}, LT'_{ij}, Φ_{ij} and Φ'_{ij} are the horizontal coordinates of the two intersection points between the ray i and the layer j.

This is a triangular linear equation system that could be solved recursively for the shape function $F(H)$ and does not require a least square fit, unlike tomographic approaches. When the TEC function is constant (spherical symmetry) equation 4 must be equivalent to the classical Abel inversion, and differences should be attributed to the numerical algorithms.

From equation 4 it is clear that, when spherical symmetry is assumed, variations in the TEC function affect the estimation of the electron density, especially if TEC presents non-linearities in the horizontal coordinates. But, even if TEC is a linear function, there is still a mismodeling related to the variation of the tangent point projection.

There are two possible scenarios in which this proposed approach could fail: (i) A change in the shape function $F(h)$ in the region of the occultation (dawn occultations, ionospheric disturbances, etc.). However, in this case the spherical symmetry approach will give a worse result because changes in the electron density function can be partially explained as changes in the TEC function. (ii) A bad estimation of the TEC could introduce a mismodeling in the estimation of the shape function that could be greater than the inherent mismodeling of the spherical symmetry assumption. Several authors (see for example *Hernandez-Pajares et al.* 1999) have shown that the TEC can be determined from ground receivers with errors below a few TECUs ($1\,TECU = 10^{16} el/m^2$), also in low latitudes and far from ground receivers; errors below 10% in the TEC.

In the implementation of this algorithm we will use as data the differences between L1 and L2 GPS carrier phases that are related with the STEC by.

$$L_I = L_1 - L_2 = \alpha \cdot STEC + b \quad (5)$$

where $\alpha = 0.105 \frac{m}{TECU}$ and b is a bias term (constant along each GPS-LEO continuous arch of data). This bias term can be eliminated by making differences with respect to a reference observation in the arch of data. Furthermore, equation 4 has to be completed with the contribution to the

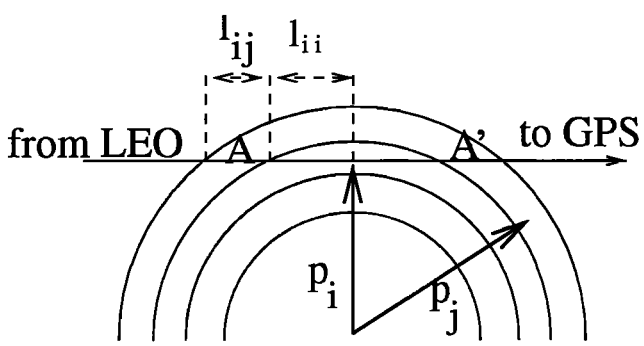

Figure 1. Layout of the inversion model geometry.

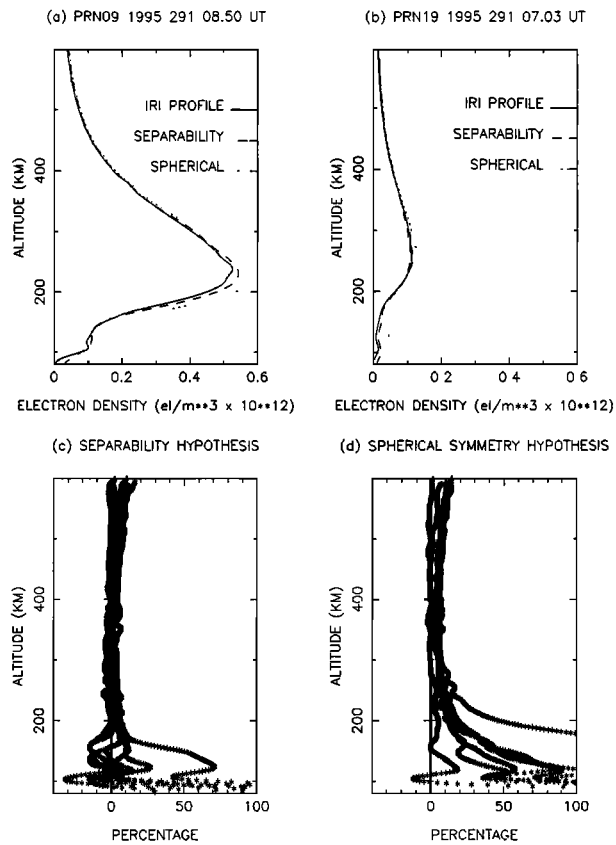

Figure 2. Electron density retrieval with simulated STEC and real geometry: Top panels, for two occultations. Bottom panels show the relative differences for all occultations, with the two tested hypotheses.

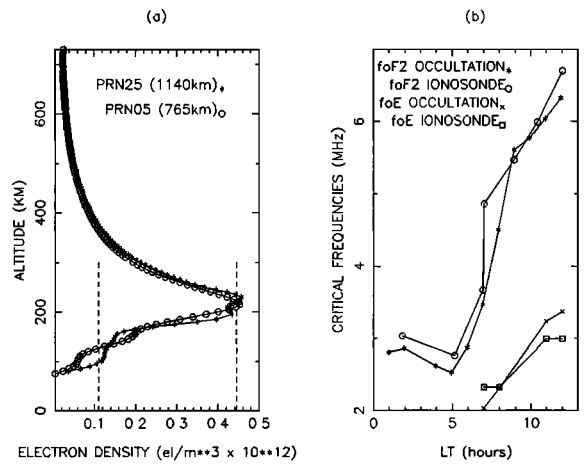

Figure 3. (a) Derived vertical profiles from GPS/MET occultation data for the Slough ionosonde at 10:00 LT. Ionosonde NmE and NmF2 values are also shown as vertical dashed lines. (b) Comparison of foE and foF2 from Slough ionosonde and the critical frequencies derived from the nearest occultation.

STEC of the ionosphere above the LEO. Then, equation 5 can be written as follows:

$$\alpha^{-1} \cdot [L_I(p_i) - L_{I(R)}] = \sum_{j=1}^{j=i-1} l_{ij} \left[TEC(LT_{ij}, \Phi_{ij}) + TEC(LT'_{ij}, \Phi'_{ij})\right] F(p_j) + 2 \cdot l_{ii} \cdot TEC(LT_{ii}, \Phi_{ii}) \cdot F(p_i) + STEC_A(p_i) - STEC_R \quad (6)$$

where $L_{I(R)}$ is the datum of the reference observation, $STEC_R$ is its STEC and $STEC_A$ is the portion of STEC above the LEO orbit. Before applying the inversion algorithm it is necessary to have a value for the difference $STEC_A(p_i) - STEC_R$. There are several ways to obtain this value: (i) if the reference observation has positive elevation each differenced STEC will have small values, so the difference can be neglected. (ii) One can choose a reference value in such a way that we can make the hypothesis that the difference is zero (this is the *calibrated STEC* of *Schreiner et al.* (1999)). (iii) Starting from one of the two preceding hypotheses (i.e. neglecting the difference) we can estimate the difference by means of an iterative procedure where the shape function is extrapolated above the LEO orbit using equation 3 as a constraint.

Results

Comparison with semi-synthetic data

In order to see the improvement of the separability hypothesis over the spherical symmetry hypothesis we make a first comparison using simulated data from an ionospheric model. With this ionospheric model we simulate both the STEC of the occultations and the VIP. We have generated two sets of semi-synthetic data (i.e. real geometry but simulated STEC as is described below) from October 18th, 1995: The first one corresponds to a set of 21 European GPS ground receivers that allow us to obtain the TEC function. The second one is a set of 7 occultations measured from the GPS/MET receiver (*Ware et al.*, 1995), working at 0.1 Hz, with tangent points in the region where the TEC is known. In both cases the rays are real receiver-GPS rays, but the STEC of each ray has been substituted by a STEC computed by an ionospheric model (in our case the International Reference Ionosphere, IRI, *Bilitza*, 1990). Thus, we can compare the results of the inversion with the known profiles of the reference model.

Figures 2a and 2b show two examples of the recovering of the model profiles in two of these occultations. In these examples, the improvement of the separability hypothesis is clear, particularly at low altitudes. Figures 2c and 2d show the fractional differences $\left(\frac{recovered\ \ density - reference\ \ density}{reference\ \ density}\right)$ for the 7 occultations with the two tested algorithms. Again, the improvement of the separability hypothesis over the spherical symmetry hypothesis is clear for all occultations. In the last case fractional errors at low altitudes are usually greater than 50% of the density values. With the proposed method these fractional differences fall below 20% also for the E layer, except for one case, where the fractional difference is greater than 50% in the E layer, although this is associated with the low reference value (see Figure 2b), but still is better than the corresponding spherical symmetry case (where the fractional difference is greater than 100%).

Comparison with real data

Two types of comparisons have been made with real data: (i) internal comparisons between close occultations, and (ii) comparisons between derived critical frequencies and close ionosonde measurements. The processed data correspond to occultations in the Northern Hemisphere on October 18th, 1995. On this date the equatorial crossing times of the LEO orbit are approximately 0000LT and 1200LT, in such a way that in the Northern Hemisphere the occultations took place between 0000LT to 1200LT. The first part of this day (European occultations) has a moderate geomagnetic activity (mean K_p index of 2.5), while in the second part of the day (North-American occultations) a geomagnetic storm occurs with K_p index from 4 to 7. The TEC function was obtained using data from 80 European and North-American IGS ground receivers following the procedure published by *Hernandez-Pajares et al.* (1999), using an horizontal grid of 5x5 degrees.

Internal comparisons The ground projection of an occultation affects to points separated by distances of several thousands of kilometers. In the spherical symmetry assumption it is supposed that all these points share an electron density function that depends only on height $N_e(h)$. By other hand, the separability hypotesis supposes that these points have the same shape function $F(h)$ in such a way that differences between electron density are explained as differences in the TEC function. A test for the self-consistency of these hypotheses can be performed by comparing the results for close occultations. This is done for occultations with horizontal distances (between its NmF2 tangent points) of less than 2000 km and time differences of less than 2 hours. In this case 30 comparisons can be made. The results in the comparisons of the derived F2 critical frequencies are shown in the second column of Table 1. Notice that the separability hypothesis gives better results than the spherical one (an improvement of 50%).

Comparison with ionosonde measurements In this comparison we use data from 29 European and North-American ionosondes. Figure 3a compares the inversion solution assuming the separability hypothesis for two occultations close to the Slough ionosonde (0.6W, 51.5N) and the electron densities, NmE and NmF2, for the E and

F2 layers measured by this ionosonde at this time. Figure 3b shows the comparison of the E and F2 critical frequencies measured from this ionosonde with the derived frequencies obtained from the nearest occultation as a function of the ionosonde local time. Notice that the worst results occur around dawn (between 0600 and 0800 LT) when the temporal/spatial variation of the F2 critical frequency is highest and the separability hypothesis (i.e. same shape function $F(h)$ for occultation and ionosonde locations) could give worse results in the transition from night to day.

The mean and rms of the fractional differences between critical frequencies from ionosondes and occultations are summarized in Table 1, columns 3 to 6. In each column the first sub-column corresponds to the separability assumption and the second sub-column corresponds to the spherical symmetry assumption. The third column corresponds to all the comparisons for the foF2 within 1 hour and 1200 km; there are 114 comparisons between ionosondes and occultations with an average distance of 850 km (22 of these comparisons occur with high geomagnetic activity without significative differences in the statistics). In the fourth column comparisons from 0600LT to 0800LT are excluded. The fifth column corresponds to the comparisons from 0600LT to 0800LT: there is a clear worsening of the results for two hypotheses due to the transition from night to day, but the separability hypothesis always provides better results. The comparison of foE (last column) is performed only when both ionosonde and occultation detect a sporadic E layer.

Discussion and conclusions

From these results it is clear that the addition of TEC information improves the results of the inversion procedure. In all cases the separability assumption provides better statistics than the traditional Abel inversion algorithm assuming spherical symmetry. This improvement is generally close to 38% in rms when ionosonde and occultation results are compared. This is true also in regions where the separability hypothesis provides worse results because of the variation of the shape function. This conclusion differs from those of *Schreiner et al.* (1999), which conclude that the Abel inversion with spherical symmetry works slightly better than the inversions using a priori densities. We think that this slight deterioration could be due to the mismodeling in the a priori densities used, which may be greater than the mismodeling in the spherical symmetry assumption. For example, the 4-D tomographic solution used as a priori density has a horizontal resolution greater than 1000 km and a vertical resolution of 120 km, these scales are clearly greater than the typical scales of an occultation discussed in this paper. The results obtained in this work show the TEC suitable as a priori information.

Using the separability hypothesis, the agreement in the detection of sporadic E is quite good (15% in rms), which is similar to percentages in the comparison of foF2 frequencies when spherical symmetry is assumed.

Finally, we have to stress that these results correspond to one day of midlatitude occultations. More data, including low and high latitude data, should be processed to confirm the improvement of this method over the classical Abel inversion.

Acknowledgments. We thanks the IGS for providing the ground receiver data, the UCAR for providing GPS/MET data and the World Data Centre for Solar-Terrestrial Physics for providing the ionosonde data. We are grateful to D. Bilitza for providing the IRI model. This work has been partially supported by the Spanish CICYT project TIC97-0993-C02-01.

References

Bilitza D., International Reference Ionosphere 1990, URSI/COSPAR, NSSDC/WDC-A-R&S 90-22, 1990.

Hajj, G. A. and L. J. Romans, Ionospheric electron density profiles obtained with GPS: Results from the GPS/MET experiment. *Radio Sci., 33(1),* 175-190, 1998.

Hajj, G.A., R. Ibanez-Meier, E.R. Kursinski, and L.J. Romans, Imaging the ionosphere with Global Positioning System, *Int. J. Imaging Syst. Technol., 5,* 174-184, 1994.

Hardy, K.R., G.A. Hajj, E.R. Kursinski, and R. Ibanez-Meier, Accuracies of atmospheric profiles obtained from GPS occultations, *Proceedings of the ION GPS-93 Conference*, 1545-1556, 1993.

Hernández-Pajares, M., J.M. Juan, J. Sanz, New approaches in global ionospheric determination using ground GPS data, *J. Atmos. Sol. Terr. Phys., 61,* 1237-1247, 1999.

Hernández-Pajares, M., J. M. Juan, J. Sanz, and J. G. Solé, Global observation of the ionospheric electronic response to solar events using ground and LEO GPS data, *J. Geophys. Res., 103, A9,* 20789-20796, 1998

Leitinger, R., H. P. Ladreiter, and G. Kirchengast, Ionosphere tomography with data from satellite reception of GNSS signals and ground reception of NNSS signals, *Radio Sci., 32(4),* 1657-1669, 1997.

Schreiner, W.S., S.V. Sokolovskiy, C. Rocken, and D.C. Hunt, Analysis and validation of GPSMET radio occultation data in the ionosphere, *Radio Sci., 34,* 949-966, 1999.

Ware, R. H., M. L. Exner, B. M. Herman, Y-H. Kuo, T. K. Meehan and C. Rocken, GPS/MET Preliminary Report, operated by the UCAR and sponsored by the NSF, the FAA and the NOAA, July 1995.

M. Hernández-Pajares, J. M. Juan and J. Sanz, Group of Astronomy and Geomatics, Universitat Politècnica de Catalunya, Campus Nord Mod. C-3, Jordi Girona 1, E08034-Barcelona, Spain. (e-mail: manuel@mat.upc.es)

(Received January 27, 2000; revised April 4, 2000;
accepted May 2, 2000.)